Evaluating the ability of a numerical weather prediction model to forecast tracer concentrations during ETEX 2

H. F. Dacre

Department of Meteorology, University of Reading, Earley Gate, PO Box 243, Reading, RG6 6BB, UK.

Abstract

In this paper the meteorological processes responsible for transporting tracer during the second ETEX (European Tracer EXperiment) release are determined using the UK Met Office Unified Model (UM). The UM predicted distribution of tracer is also compared with observations from the ETEX campaign. The dominant meteorological process is a warm conveyor belt which transports large amounts of tracer away from the surface up to a height of 4 km over a 36 hour period. Convection is also an important process, transporting tracer to heights of up to 8 km. Potential sources of error when using an operational numerical weather prediction model to forecast air quality are also investigated. These potential sources of error include model dynamics, model resolution and model physics. In the UM a semi-Lagrangian monotonic advection scheme is used with cubic polynomial interpolation. This can predict unrealistic negative values of tracer which are subsequently set to zero, and hence results in an overprediction of tracer concentrations. In order to conserve mass in the UM tracer simulations it was necessary to include a flux corrected transport method. Model resolution can also affect the accuracy of predicted tracer distributions. Low resolution simulations (50 km grid length) were unable to resolve a change in wind direction observed during ETEX 2, this led to an error in the transport direction and hence an error in tracer distribution. High resolution simulations (12 km grid length) captured the change in wind direction and hence produced a tracer distribution that compared better with the observations. The representation of convective mixing was found to have a large effect on the vertical transport of tracer. Turning off the convective mixing parameterisation in the UM significantly reduced the vertical transport of tracer. Finally, air quality forecasts were found to be sensitive to the timing of synoptic scale features. Errors in the position of the cold front relative to the tracer release location of only 1 hour resulted in changes in the predicted tracer concentrations that were of the same order of magnitude as the absolute tracer concentrations.

Key words: pollution transport, mass conservation, UK Met Office Unified Model

1. Introduction

To predict the evolution of chemical species in the atmosphere it is important to understand both the chemistry and the dynamical processes responsible for their dispersion. Many chemistry transport models (CTMs) have been developed to forecast the dispersion of trace gases and aerosols. The operation of a CTM involves first running a numerical weather prediction (NWP) model independently of the CTM. The NWP output is typically archived every 1 to 12 hours and is used to drive the transport in the CTM. This method relies on the fundamental assumption that the variability present in the meteorological fields is represented in the archived data (Korsholm et al., 2009). Within the atmosphere high frequency variability is generated by mesoscale and microscale flows such as orographic flows, sea breezes, frontal circulation, boundary layer turbulence and moist convection. The rapid changes in wind speed and direction, cloud formation and rainfall associated with these processes can be absent in archived meteorological data as the time scale and spatial scale of these processes is often less than the intervals at which data is archived for use with a CTM (Rasch et al., 1997). The accuracy of CTM predictions has been found to be sensitive to the frequency of the meteorological input in studies by Brost et al. (1988), Nasstrom and Pace (1998), Rasch et al. (1997), Grell et al. (2004) and Davis and Dacre (2009). Improvement in the accuracy of CTM predictions due to high frequency coupling intervals has been found and is more evident when the meteorological fields involve mesoscale circulations (Brost et al., 1988; Fay et al., 1995). However, large amounts of data storage are required by applying one model after the other if the high frequency variability is to be captured. In addition, if archived data is sampled instantaneously important transient events may be missing. Alternatively, if archived data is averaged there will be a lack of extreme events in the data.

To avoid the problem of archiving large amounts of NWP output it is possible to reproduce the high frequency variability in the meteorological fields by representing transport by processes occuring at unresolved time scales and spatial scales within the CTM itself (Korsholm et al., 2009). The effect of sub-grid processes on the large-scale can be represented statistically. However, there is not always enough data in the archive to do this parameterisation well. One further disadvantage of operating CTMs independently of the meteorology is that there is no possibility to consider the interaction between the meteorological fields and chemistry (e.g. interaction between aerosol and precipitation and cloud condensation nuclei or interaction between aerosols and radiation) which can be significant on regional scales.

Increases in computing power now enable us to use high resolution NWP models to explicitly resolve both synoptic scale features as well as mesoscale features such as frontal circulations, convection, local wind flows and even clouds. It also allows us to perform integrated NWP-CTM calculations thus providing meteorological fields at each model timestep, typically every 5 to 10 minutes at high spatial resolution (grid lengths $\approx$ 10 km), and allows potential feedbacks between meteorological fields and chemistry. However, NWP-CTMs are more complex than existing CTMs and have not been subject to the same degree of testing applied to short range dispersion models. In this paper the dispersion of tracer simulated by an NWP model is investigated in order to determine the potential ability and limitations of NWP-CTM models to accurately predict the dispersion of pollutants.

The aim of this paper is to assess the performance of the UK Met Office's NWP Unified Model (UM) in predicting tracer concentrations across Europe. Specific attention is paid to the meteorological processes (such as frontal flows and convection) in both local and long-range transport. The tracer distributions in the UM are compared with observations from the European Tracer EXperiment (ETEX). The ETEX field campaign is described in section 2. The model used in this paper is described briefly in section 3. In section 4 an analysis of the meteorological fields during the second ETEX release is given. The observations from the ETEX field campaign are described in section 5 and they are compared with the UM tracer experiment in section 6. Potential sources of error in the UM tracer experiment are also described in section 6. Finally, in section 7 the main conclusions are given.

2. The European Tracer Experiment

Two long-range dispersion experiments were carried out as part of ETEX during October and November 1994. During the releases, a non-toxic, non-depositing, inert tracer (perfluoromethylcyclopentane) was released from a site near Monterfil in north-west France ($12°00'30''$ W, $40°03'30''$ N). 168 stations, all part of the synoptic network of national meteorological services, in 17 countries were equipped with air samplers and performed 3 hourly sampling (figure 1). A complete description of the ETEX experiment was published by Van Dop et al. (1998) and Gryning (1998).

Since the release rate was well known and deposition and chemical processes did not occur the experiment provides a good test of atmospheric transport in models from a point source at continental scale. 24 institutions took part in real-time forecasting of plume evolution, with 28 long-range CTMs, using meteorological data from various sources. The first ETEX experiment (ETEX 1) has been discussed in many papers in which the modelling results have been compared to observations (Ryall and Maryon, 1998; Stohl et al., 1998; Nasstrom and Pace, 1998; D'Amours, 1998). It was concluded in a review paper by Mosca et al. (1998) that almost all the models showed a satisfactory agreement with the measured values for ETEX 1.

However, for the second ETEX experiment (ETEX 2) the models did not perform as well. The synoptic situation was similar to the first release, with a low between Iceland and Norway moving eastwards and decaying. However, unlike the first release, in which the meteorological fields near the source remained fairly constant throughout the release, the second release was made into strong winds and continued though a cold-front passage. The more complex meteorological situation, involving mesoscale circulations, made the evolution of the tracer plume more difficult to predict. Van Dop et al. (1998) in their review paper concluded that all models significantly over-predicted surface concentrations and that no clear explanation was given for this result. As a typical example, Ryall and Maryon (1998) found that the Lagrangian dispersion model (Numerical Atmospheric-dispersion Modelling Environment, NAME), driven by 50 km grid length resolution meteorological data input at 3 hourly time intervals severely over-predicted surface concentrations, especially during the first 24 hours. In addition, during the second 24 hours the observations were to the west of (behind) the predicted plume. They hypothesised that the failure of the meteorological input data to represent the drop in wind speed and change in wind direction associated with the passage of the cold front led to a misprediction in the plume direction. Stohl et al. (1998) using another Lagrangian CTM (FLEXPART) found similar results and that surprisingly the model performance did not deteriorate with time (a similar result was also found by Davis and Dacre (2009) using NAME). More recently, Krysta et al. (2008), using an Eulerian CTM (POLAIR3D), concluded that the observational data exhibited inconsistencies during the early evolution of the plume, suggesting the measurements may be incorrect.

To summarise, all of the models that took part in the prediction of ETEX 2 over-predicted surface concentrations and failed to capture the plume location at later times. In this paper model simulations are performed using an NWP model with high frequency meteorological fields and a state-of-the-art convective parameterisation scheme. Simulations are performed at two horizontal resolutions to determine whether a better representation of the cold front and mesoscale processes results in a more accurate forecast of tracer distribution.

3. UM description and methodology

Simulations of the ETEX 2 release have been performed the UK Met Office Eulerian NWP model, UM, version 6.1. This model solves the non-hydrostatic primitive equations using a semi-implicit, semi-Lagrangian numerical scheme (Cullen , 1993; Davies et al. , 2005). The model includes a comprehensive set of parameterisations, including boundary layer turbulent mixing (Lock et al. , 2000), mixed phase microphysics (Wilson and Ballard , 1999) and convection (Gregory and Rowntree , 1990). There is no explicit horizontal diffusion in the model. A limited area domain with horizontal grid length of 0.442° (approximately 50 km) and 0.11° (approximately 12 km) was used over Europe extending from 37.5° N to 62.47° N and 9.5° W to 22.62° E. The model has 38 levels in the vertical on a stretched grid ranging from the surface to 5hPa. This corresponds to approximately 100 m layer spacing in the boundary layer and 500 m layer spacing in the mid-troposphere. The first model level is at 20 m. The 50 km grid length UM has a timestep of 10 minutes and the 12 km grid length UM has a timestep of 5 minutes.

The tracer release is represented in the UM by a constant emission of tracer into the lowest model gridbox. The release rate is chosen to be equivalent to 11.58 g s^{-1}. Tracers in our simulation are treated as passive substances, they are subject to advection, convection and turbulent transports but are neither deposited nor chemically transforming. A small amount of transport may occur due to numerical diffusion. This methodology has also been used by Donnel et al. (2001); Gray (2003); Augusti-Panareda et al. (2005); Dacre et al. (2007).

4. ETEX 2 meteorology

Before performing a simulation of the tracer transport that took place during the ETEX 2 release, it is important to identify the meteorological processes occuring on this day that could be responsible for transporting pollution.

The ETEX 2 tracer release took place between 15 UTC on 14 November and 02:45 UTC on 15 November 1994. Figure 2(a) shows the frontal analysis for 00 UTC on 13th to 16th November 1994. A mature low pressure system, 970hPa, was located north of the UK and approached Europe from the west. A frontal wave in the cold front delayed the frontal passage over the release site which occurred at approximately 02 UTC on 15 November 1994. Figure 2(b) shows a visible image from the Modis Aqua satellite at 07:50 UTC on 14 November 1994. The main polar-front cloud band lies south of the low pressure centre parallel to and ahead of the surface cold front and wraps cyclonically around the low pressure centre.

4.1. Wind speed and Wind direction

It is necessary to model wind direction accurately as tracer concentration fields are very sensitive to transport direction, since small errors can be the difference between a tracer impacting or missing a receptor site. Wind speed is also important as the transport speed determines the timing of the tracer impact and the horizontal and vertical dispersion of a plume which is critical for properly simulating the plume concentration at a receptor site (Schichtel et al., 2005). In this section the UM simulated wind speed and direction at two horizontal grid lengths, 50 km and 12 km, are compared with the observed wind speed and direction measured at the release site.

Figures 3(a) and (b) show the time evolution of the wind speed and wind direction at the tracer release site respectively. The wind was measured using a sonic anemometer and averaged over 10 minute intervals, hourly averages are also calculated for comparison with the UM data. The observations show that prior to the passage of the front the wind speeds were between 8 and 10 m s^{-1} with a wind direction of 230°. As the front passed over the release site there was a drop in wind speed from 8 to 2 m s^{-1} and a very sharp change in wind direction from 250° to 320° occuring over a 10 minute period. Behind the cold front, the wind speed gradually increased from 2 to 4 m s^{-1} and the wind direction remained roughly constant at 280°. Comparing the hourly averaged observed wind speed with the UM simulations, figure 3(a), we see that ahead of the cold front both the 12 km and 50 km grid length simulations underestimate the observed wind speed, with the low resolution simulation performing slightly better than the high resolution simulation. As the cold front passes over the release site (between 02 and 04 UTC on 15 November 1994) both the high and low resolution simulations capture the drop in wind speed seen in the observations. Behind the cold front, both simulations again underestimate the observed wind speed but this time the high resolution simulation is closer to the observed wind speed than the low resolution simulation. Comparing the observed wind direction with the UM simulations, figure 3(b), we see that ahead of the cold front both the high and low resolution simulation estimates of the wind direction closely match the observations. However, as the cold front passes over the release site the observed sharp change in wind direction is not captured by the low resolution simulation, which shows the change occuring over a 6 hour period. The high resolution simulation does represent the observed sharp change in wind direction, but it appears to be delayed in the simulation by an hour or more.

4.2. Warm conveyor belt

Figure 4(a) shows the wet-bulb potential temperature at 850 mb at 03 UTC on 15 November 1994. The cold front associated with the low-pressure system extends from the Bay of Biscay, to Sweden and Norway. The warm front extends from Switzerland up to Sweden. Warm moist air exists between the cold and warm front in the cyclone's warm sector. Figure 4(b) shows the 3-hourly averaged (0 to 3 UTC 15 November 1994) large-scale rain amount. The pattern of large-scale rain matches closely the shape of the polar front cloud band shown in the satellite image in figure 2(b). The large-scale rain occurs as a result of warm moist air ascending along the warm conveyor-belt flow in the warm sector of the cyclone. Figure 4(c) shows the 3-hourly averaged convective rain amount. An intense band of convection is observed to lie along the cold front in the model simulation. It will be shown in section 6 that the location of these convective cells is aligned along the direction of the tracer plume axis and that they are responsible for transporting tracer out of the warm conveyor-belt flow, up to 8 km in the atmosphere.

In order to determine the three-dimensional warm conveyor belt flow isentropic surface analysis was performed relative to the moving system. When air ascends adiabatically its potential temperature remains constant so ascending air may be considered as flowing along a constant potential temperature (i.e. isentropic) surface. Wet-bulb potential temperature, θ_w, surfaces describe the flow of saturated air. For the frontal system, the air ahead of the cold front is largely saturated so wet-bulb potential temperatures have been used to describe the flow. Isentropic analysis is carried out relative to the moving system assuming that the system is moving with a constant speed. The system relative velocity is computed by subtracting the system velocity from the local wind vectors. This is known as 'relative flow isentropic analysis' (Browning and Roberts , 1994). The system speed was defined as the average speed that the low pressure centre travelled during the period 00 UTC on 14 November to 00 UTC on 16 November 1994. The frontal cyclone was travelling with a component of 14.2 m s^{-1} toward the east and 2.6 m s^{-1} towards the north. Isentropic surface analysis has been carried out on the frontal cyclone. The isentropic surface shown in figure 5 is the $\theta_w = 288°$ K moist isentropic surface. This shows a flow corresponding to part of the warm conveyor-belt, ascending sharply from 500 m in the warm sector to 4 km ahead of the warm front. The air then continues to rise up to 6 km while turning cyclonically. The warm conveyor belt flows from low levels over the warm front to mid-levels forming the polar front cloud band. The structure of this flow compares well with the classical conceptual model of the warm conveyor belt described in Browning and Roberts (1994). It will be shown in section 6 that the ascent in this warm conveyor-belt flow is responsible for transporting large amounts of tracer away from the surface up to 4 km.

5. Observed tracer transport

In this section the observed tracer concentrations from the ETEX 2 experiment are described. Because an existing network was used there were some limitations in the spatial resolution of the sampling. For example, the resolution of the sampling network close to the release site was too coarse to properly resolve the near-source dispersion (Mosca et al., 1998). The observations have been gridded onto a 50 km × 50 km grid for ease of comparison with the UM simulations.

Figure 6(a) shows the observed tracer 12 hours after the start of the tracer release. During the first 12 hours, low concentrations of tracer (< 2 ng m^{-3}) were advected rapidly to the north-east by strong surface winds. The split nature of the plume at this stage is likely to be a result of the sparse measurement network. Figure 6(b) shows the observed tracer distribution 24 hours after the start of the tracer release. At this time the plume had split into two distinct regions. There is an area of tracer observed close to the release location, in France, and another region further north and east over Poland and the Czech Republic. Small amounts of tracer were also observed at isolated locations in between these two main regions. Finally, figure 6(c) shows the observed tracer distribution 36 hours after the start of the tracer release. By this time most of the observed tracer remained in France, with small amounts over Switzerland and Germany. It is hypothesised that tracer observed in Poland and the Czech Republic after 24 hours has been advected out of the measurement network by this time.

There was considerable surprise from the measurement and modelling communities who participated in the ETEX campaign, both as to the low concentrations of tracer observed and to the relatively few number of stations that observed tracer during the ETEX 2 release. As described in section 2, all of the models overpredicted the magnitude of the observed tracer concentrations and also failed to predict the slow moving tracer that remained for a long period in western Europe.

6. UM tracer transport

In this section the tracer transport predicted by the UM is presented and compared with the ETEX observations. Potential sources of error when using the UM as an air quality forecast model are also described.

6.1. Model dynamics - tracer mass conservation

The UM uses a semi-Lagrangian monotonic advection scheme with a cubic polynomial interpolation to predict the evolution of its dynamical fields and the evolution of tracer fields. As a result, the release of tracer over a single gridbox can cause problems as near sharp gradients of tracer concentration unrealistic negative values of tracer can be predicted. As the advection scheme is monotonic, no new extrema in tracer concentrations can be introduced. Thus negative values of tracer, produced by the polynomial interpolation scheme, are set to zero causing a lack of mass conservation. Such behaviour is likely to have a detrimental effect on any field with sharp gradients, such as moisture, and is unacceptable for air pollution modelling, where mass conservation is of high importance and the gradients are very large close to source locations. Before carrying out a simulation of ETEX 2 using the UM a sensitivity study has been performed to look at the tracer mass conservation properties of the UM.

Figure 7 shows the time evolution of the total mass of tracer in the 12 km grid length UM simulation using various sized emission areas. In all of the simulations the tracer is released from 15 UTC on 14 November until 02:45 UTC on 15 November 1994. The total mass of tracer should increase linearly between these times and then remain constant for the remainder of the simulation at a value equal to the total emitted tracer mass. The size of the area over which tracer was emitted has been varied from 1 single gridbox (equivalent to a 12 km$\times$12 km area) to a 9x9 area of gridboxes (equivalent to a 108 km$\times$108 km area). For the single gridbox release, the total amount of tracer increases too fast during the duration of the tracer release and continues to increase after the end of the release for a further 3 hours before reaching its maximum amount, which is 2.5 times the total emitted mass. Increasing the size of the emission area reduces the excess tracer in the simulation because undershoots in concentration are minimized due to less steep concentration gradients. For the 9x9 gridbox emission the percentage error in total tracer by the end of the simulation is approximately 15%. To improve the mass conservation properties of the UM the flux corrected transport method of Priestley (1993) is implemented. The Priestley (1993) flux corrected transport method involves predicting the solution by both the cubic polynomial interpolation scheme and the linear interpolation scheme. The Priestley (1993) method then locally detects the regions of large interpolation error, performs the mass correction without a violation of the monotonicity, and gives the best solution in discontinuous regions, thus conserving tracer mass. Figure 7 shows the mass conservation of a single gridbox release with the Priestley conservation scheme turned on. 100% of the tracer mass is conserved during the emission of tracer. The slight decrease in tracer amount towards the end of the simulation is due to tracer being advected out of the domain. Thus, the Priestley conservation scheme is turned on for the UM simulations described in sections 6.2 to 6.4.

6.2. Model Resolution

The simulation of tracer transport for ETEX 2, carried out using the UM with 50 km grid length is shown in figure 8(a) to (c). Figure 8(a) shows the distribution of tracer in the lowest model grid box, 12 hours after the start of the tracer release. The tracer has been transported north-eastwards by the low-level winds. Modelled wind strengths in the lowest model grid box at the release site were between 8 and 9 m s^{-1} ahead of the cold front, with a constant wind direction of 225°, figure 3(a) and (b). The plume width in the lowest model grid box is approximately 500 km and extends approximately 1000 km from the release site, with tracer concentrations (> 4 ng m^{-3}) extending 300 km from the release site. 24 hours after the start of the tracer release, figure 8(b), the low-level tracer plume now extends further, 1700 km from the source location, and is orientated in a more easterly direction. 36 hours after the start of the tracer release, figure 8(c), the plume has continued to be transported to the east, now extending well over 2000 km in length.

The simulation of tracer transport for ETEX 2 carried out using the UM with 12 km grid length is shown in figures 8(d) to (f). Figure 8(d) shows the distribution of tracer in the lowest model grid box, 12 hours after the start of the tracer release. Comparing this to the 50 km grid length simulation at the same time, figure 8(a) we see that the orientation and distance from the source travelled by the plume is similar in the two simulations reflecting the similar wind speed and wind directions in the two models ahead of the cold front, figures 3(a) and (b). The width of the plume in the high resolution simulation is approximately 170 km, a third of that in the low resolution simulation. By 24 hours, figure 8(e), there is a difference in the location of the maximum tracer concentration. In the high resolution simulation, the maximum tracer concentration occurs 70 km south of the maximum tracer concentration in the low resolution simulation. By 36 hours after the start of the tracer release, figure 8(f), the maximum tracer concentration in the high resolution simulation is 150 km further south than the maximum tracer concentration found in the low resolution simulation.

In summary, increasing the horizontal resolution of the UM results in a tracer distribution that is narrower in the cross-wind direction than the low resolution simulation. There is also a large difference in the location of the maximum tracer concentration. Comparison with the observations, figures 6(a) to (c), shows that the high resolution UM simulation predicts a tracer distribution that is closer to the observed distribution than the low resolution simulation, especially after 24 hours. This is due to a more accurate representation of the change in wind direction associated with the cold front. These results are consistent with Davis and Dacre (2009) who showed that increasing the horizontal resolution of the meteorological data used to drive the UK Met Office dispersion model, NAME, resulted in a statistically significant improvement in the model simulation after 24 hours, although little difference was seen at earlier times. Both the UM and NAME however, still overpredict the observed tracer concentration. It is hypothesised that the ascent in the warm conveyor belt is too weak in both of the UM simulations for ETEX 2 leading to an over prediction of surface concentrations.

6.3. Model physics - convective parameterisation

To determine the vertical distribution of tracer cross-sections were taken through the tracer plume in the 12 km UM simulation. The position of these vertical cross-sections are shown in figures 8(d) to (f). Their orientations have been chosen to intersect the column of maximum tracer concentration, which tends to be orientated in a more easterly direction than the plume orientation in the lowest model grid box, i.e. the plume turns anticyclonically with height.

Figure 9(a) shows a vertical cross-section of tracer concentration in the 12 km grid length UM simulation 12 hours after the start of the tracer release. Much of the tracer has been lifted away from the surface along the 287 K and 288 K moist isentropic surfaces up to 2.5 km. Figure 9(b) shows a vertical cross-section of tracer concentration in the 12 km grid length UM simulation 24 hours after the start of the tracer release. By this time the tracer has formed a layer of high concentration between 2 km and 4 km. The wet-bulb potential temperatures can be used to identify the location of the surface warm and cold fronts. The maximum tracer concentrations for tracer released ahead of the cold front is found at elevated levels whereas the maximum tracer concentrations for tracer released behind the cold front is trapped near the surface. Figure 9(c) shows a vertical cross-section of tracer concentration in the 12 km grid length UM simulation 36 hours after the start of the tracer release. The separation of the pre-frontal released tracer and post-frontal released tracer is again evident with the elevated tracer remaining close to the 287 K moist isentrope.

Figure 10(a) again shows a vertical cross-section of tracer concentration in the 12 km grid length UM simulation 36 hours after the start of the tracer release but this time taken through a layer which intersects tracer at levels above 6 km. It can be seen that tracer has been transported up to 8 km in the model. Figure 10(b) shows the same cross-section as figure 10(a) but the tracer in this simulation has been prevented from going through the convection scheme. In this simulation, there is no tracer transported above 6 km in the atmosphere. The magnitude of tracer in the elevated layer between 2 km and 4 km, that has been transported by the warm conveyor belt, is slightly larger as a result.

In summary, as early as 12 hours after the start of the tracer release, most of the tracer has been lifted away from the surface by the warm conveyor belt and forms a layer aloft. The tracer is lifted to form a layer between 2 km and 6 km. Tracer is transported higher up to 8 km in the atmosphere by convection. Unfortunately, there are no above-surface measurements available to evaluate these model results. However, this study does show that the vertical distribution of tracer is sensitive to the representation of sub-grid scale processes, such as convection, and hence potentially an incorrect representation of subgrid scale processes in the model physics can lead to errors in the prediction of tracer concentration.

6.4. Timing of synoptic features

Figure 3(b) suggests that the timing of the frontal passage over the release site was delayed in the UM simulation by 1 hour or more. The rapid change in wind direction occurs 1 hour earlier in the observations than in the high resolution UM simulation. This could result in less tracer being transported vertically in the strong updraughts associated with frontal line convection and also result in less time spent within the warm-conveyor belt leading to an over-prediction of near surface concentrations.

A simulation was performed in which the tracer release was delayed by 1 hour, i.e. the start of the tracer release was 16 UTC on 15 November 1994. The duration of the tracer release remained at 11 hours 45 minutes. Figure 11(a) shows the difference in tracer concentrations in the lowest model grid box between this simulation and the original simulation 12 hours after the start of the tracer release (i.e at 03 UTC for original simulation and 04 UTC for delayed simulation). Figure 11(a) shows a dipole of negative and positive tracer anomalies of similar magnitude. This indicates that the location of the delayed tracer plume lies just to the south of the original plume. The change in plume orientation is a result of the 8° veer in wind direction that occurs between 16 UTC on 15 November and 03 UTC on 16 November 1994 as the cold front approaches (figure 3(b)). Figure 11(b) shows the difference in tracer concentrations 24 hours after the start of the tracer release (i.e at 15 UTC for the original simulation and 16 UTC for the delayed simulation). At this time the pattern of negative and positive tracer anomalies is similar to the pattern after 12 hours. However, delaying the release by 1 hour results in more tracer being transported to the southeast at a slower speed than in the original simulation as a result of the decrease in wind speed and change in wind direction behind the cold front, figures 3(a) and (b). Finally, figure 11(c) shows the difference in tracer concentrations 36 hours after the start of the tracer release (i.e at 03 UTC on 16 November 1994 for the original simulation and 04 UTC on 16 November 1994 for the delayed simulation). The largest differences are seen at the westward extent of the tracer plume where a large positive anomaly is found. This is a result of more tracer in the delayed simulation being transported slowly behind the cold front than in the original simulation.

To summarise, errors in the position of the cold front relative to the tracer release location of only 1 hour can result in changes in the predicted tracer concentrations that are of the same order of magnitude as the absolute tracer concentrations. This emphasises the point that errors in the positioning of meteorological phenomena such as fronts can result in very large changes in the distribution of tracer.

7. Conclusions

The UK Met Office Unified Model has been used to determine the meteorological processes that influenced transport during the second ETEX tracer release which took place on 14 November 1994. On this day a passive tracer was released from a site in north-west France into strong winds and continued through a cold-front passage. UM simulations show that tracer released ahead of the cold front was transported north-eastwards by strong surface winds and that a warm conveyor belt, ahead of the cold front, was responsible for transporting large amounts of tracer away from the surface up to heights of 4 km. Tracer was transported further to a height of 8 km by convection. Tracer released behind the cold front was transported more slowly eastwards and remained trapped near the surface.

Tracer distributions predicted by the UM for the ETEX 2 release were evaluated against observed tracer concentrations. It was found that high resolution UM simulations were needed to correctly predict the observed tracer distribution. This is due to a more accurate representation of the mesoscale processes, in particular the rapid change in wind direction associated with the cold front. Vertical tracer distributions predicted by the UM with and without tracer passing through the convection scheme were compared. It was found that the convection scheme in the UM transported tracer up to 8 km. Thus, the representation of convective transport in NWP models can potentially affect the distribution of tracer and lead to errors in tracer distribution. Finally, the distribution of tracer was found to be very sensitive to the position of synoptic scale features relative to the position of the release location. Small changes in the timing of the cold front passage in the ETEX 2 simulation resulted in large differences in the distribution of tracer. These differences were of the same order of magnitude as the absolute tracer concentrations. Thus, accurate positioning of synoptic scale features is essential to correctly predict tracer concentrations.

In conclusion, it is possible to simulate the transport of pollution using the UK Met Office NWP model, however it was found that the accuracy of air quality forecasts using the UM are sensitive to the choice of model dynamics, model physics, model resolution as well as the accuracy of the meteorological forecast.

8. Acknowledgements

I would like to thank the UK Met Office for use of the UM and NAME and Stefano Galmarini for providing the ETEX tracer measurements. I am grateful to Lois Steenman-Clark and William McGinty for help with the UM. I also thank Suzanne Gray and Jeffrey Chagnon for many useful discussions about this work.

References

A. Augusti-Panareda, S. L. Gray and J. Methven (2005), Numerical modeling study of boundary-layer ventilation by a cold front over Europe, J. Geophys. Res., 110, D18304, doi:10,1029/2004JD005555.

R. A. Brost, P. L. Haagenson and Y. -H. Kuo (1988), Eulerian simulation of tracer distribution during CAPTEX, J. Appl. Met., 27, 579-593.

K. A. Browning and N. M. Roberts (1994), Structure of a frontal cyclone, Q. J. R. Meteorol. Soc., 120, 1535-1557.

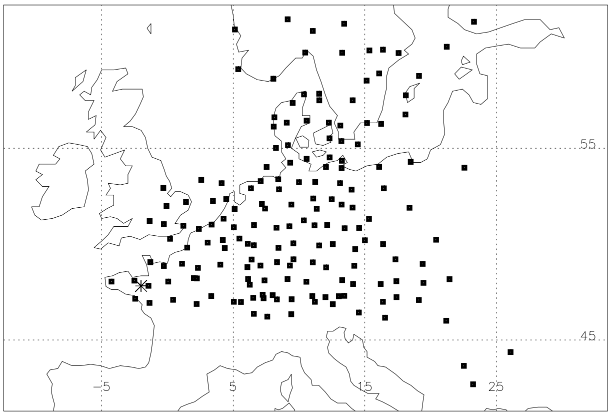

Figure 1: Surface measurement locations. The star indicates the location of the release site.

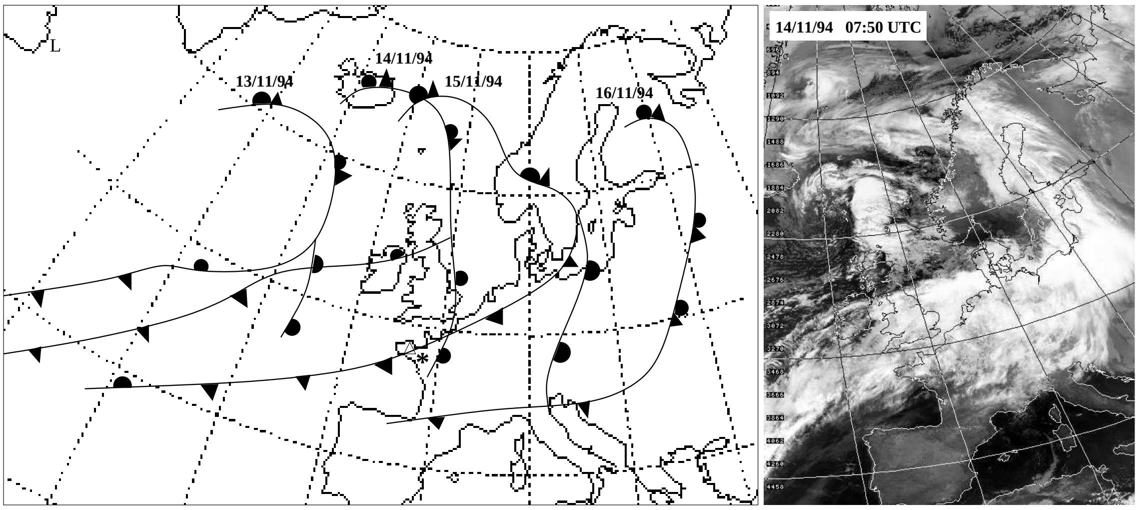

(a) (b)

Figure 2: (a) Frontal analysis at 00 UTC on 13th, 14th, 15th and 16th November 1994 and (b) visible image from the Modis Aqua satellite at 07:50 UTC on 14 November 1994. Courtesy of NASA Goddard Space Flight Centre. The star indicates the location of the release site.

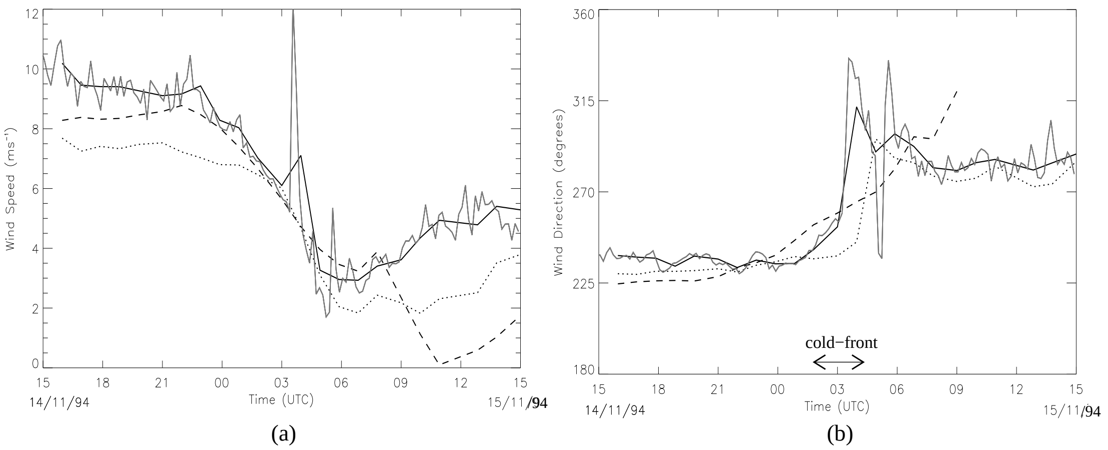

Figure 3: Time evolution of (a) wind speed and (b) wind direction at the tracer release location. 10-minute averaged sonic anemometer measurements (grey solid), 1-hour averaged sonic anemometer measurements (black solid), 50 km grid length UM simulation (dashed), 12 km grid length UM simulation (dotted). Wind direction has not been plotted when wind speed is below 1.5 m s^{-1}.

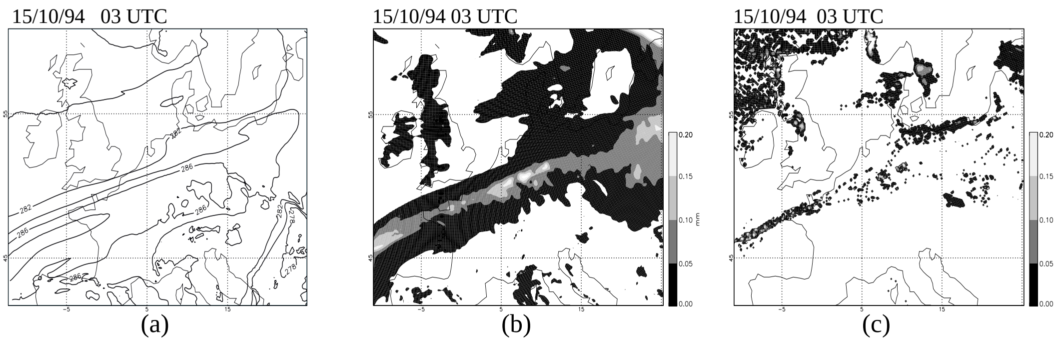

Figure 4: Model-simulated fields from the 12 km grid length UM run, at 03 UTC on 15 November 1994. (a) Wet-bulb potential temperature at 850 mb, contours every 2 K, (b) 3-hourly averaged large-scale precipitation amount, (c) 3-hourly averaged convective precipitation amount.

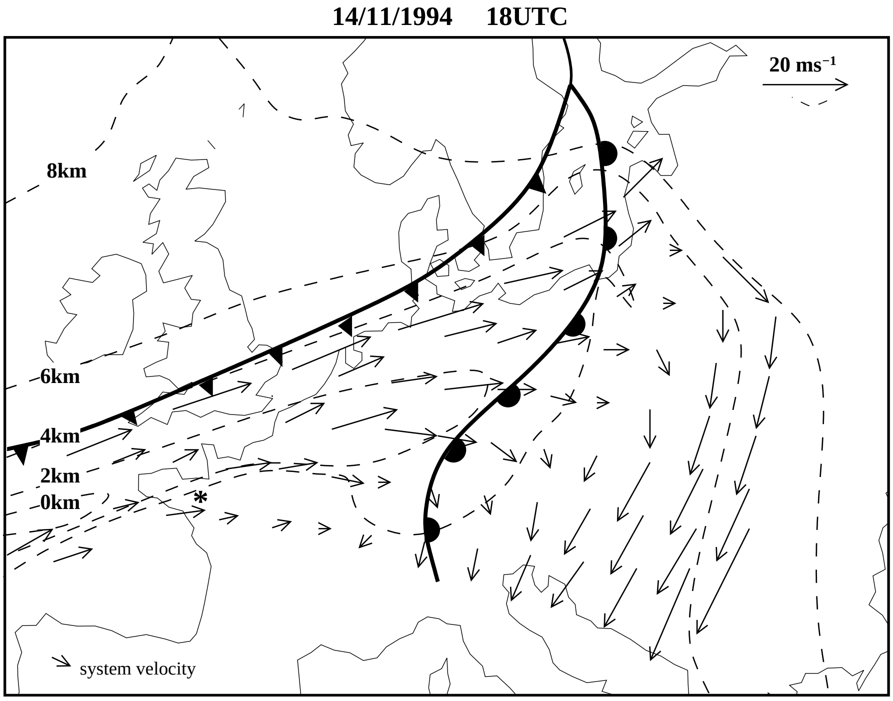

Figure 5: Model-simulated moist isentropic flow relative to the frontal cyclone from the 12 km grid length UM run at 18 UTC on 14/11/1994. Flow on the $\theta_w = 15°$C surface. Relative flow (arrows) and height of that surface at 500 m intervals (dashed contours). Surface cold and warm fronts overlaid.

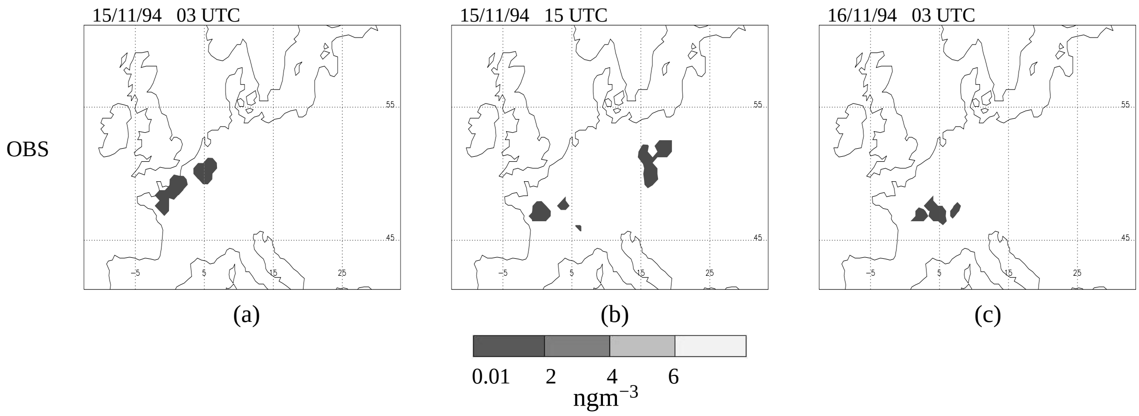

Figure 6: Observed tracer at (a) 03 UTC on 15 November 1994, (b) 15 UTC on 15 November 1994 and (c) 03 UTC on 16 November 1994.

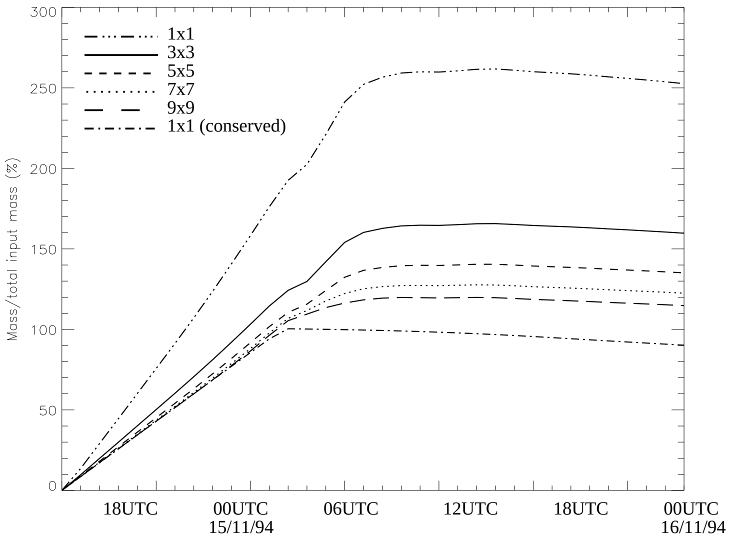

Figure 7: Time evolution of the total amount of tracer in the 12 km grid length UM. Release over 1 gridbox (dash-dot-dot-dot), 3x3 gridboxes (solid), 5x5 gridboxes (dashed), 7x7 gridboxes (dotted), 9x9 gridboxes (long-dashed), UM conserved tracer (dash-dot).

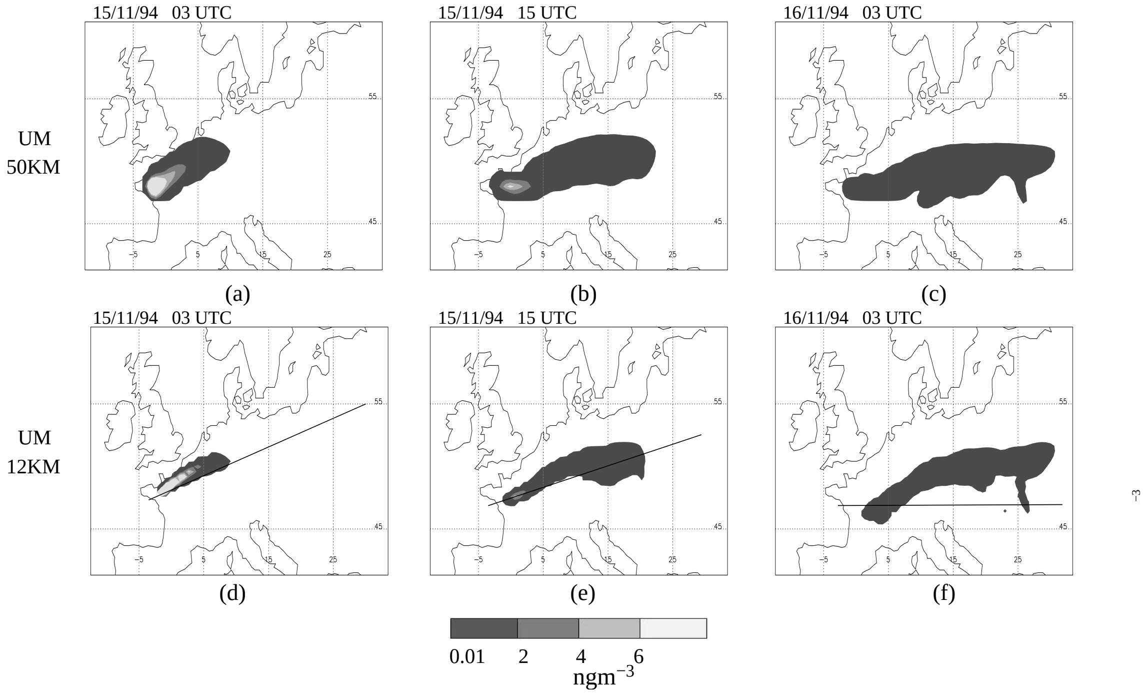

Figure 8: UM tracer concentration simulated using 50 km grid length UM (a) to (c) and 12 km grid length UM (d) to (f). (a),(d) 03 UTC on 15 November 1994, (b),(e) 15 UTC on 15 November 1994 and (c),(f) 03 UTC on 16 November 1994. Solid lines represent the location of the vertical cross-sections shown in figures 9(a) to (c).

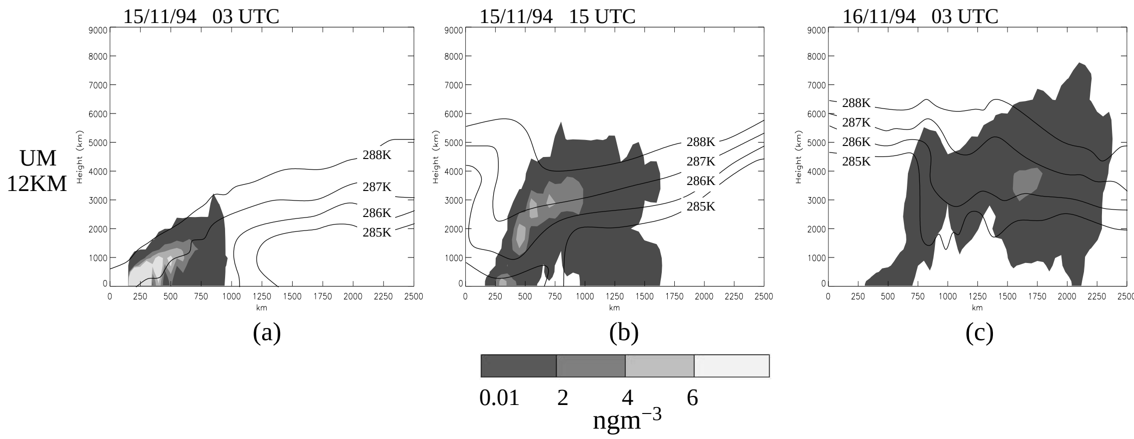

Figure 9: Vertical cross-sections of tracer concentration simulated using 12 km grid length UM overlaid with 285-288 K moist isentropes (a) 03 UTC on 15 November 1994, (b) 15 UTC on 15 November 1994 and (c) 03 UTC on 16 November 1994.

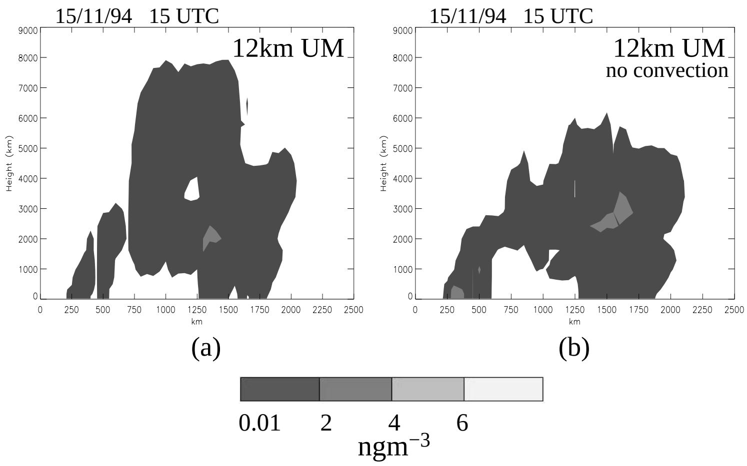

Figure 10: Vertical cross-sections of tracer concentration at 03 UTC on 16 November 1994 simulated using (a) 12 km grid length UM with convective parameterisation on, (b) 12 km grid length UM with convective parameterisation off.

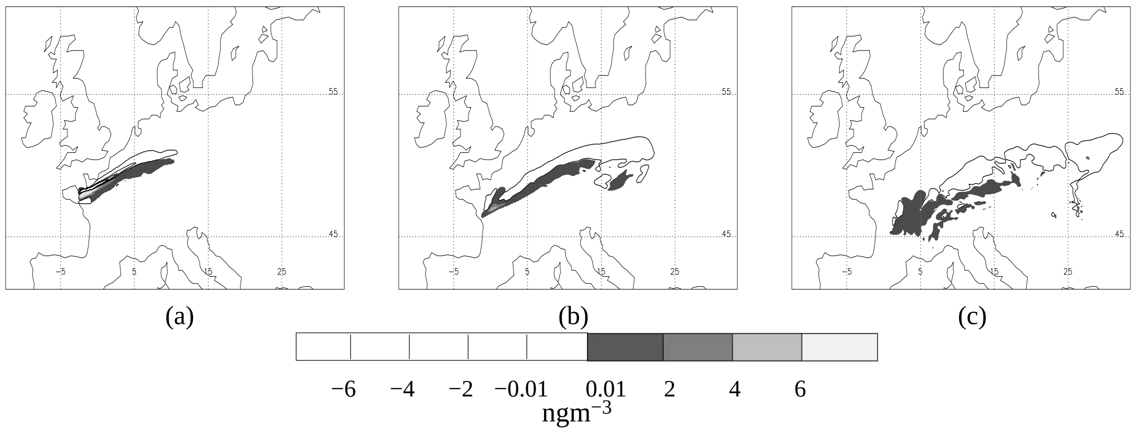

Figure 11: 12 km grid length UM tracer concentration difference between the simulation in which the release was delayed by 1 hour and the original simulation. Positive differences (colour filled contours), negative differences (unfilled contours). (a) 03 UTC on 15 November 1994, (b) 15 UTC on 15 November 1994 and (c) 03 UTC on 16 November 1994.

M. Cullen (1993), The unified forecast/climate model, Meteorol. Mag., 122, 81-94.

H. F. Dacre, S. L. Gray and S. E. Belcher (2007), A case study of boundary layer ventilation by convection and coastal processes, J. Geophys. Res., 112, D17106, doi:10.1029/2006JD007984.

R. D'Amours (1998), Modeling the ETEX plume dispersion with the Canadian emergency response model, Atmos. Env., 32, 4335-4341.

L. S. Davis and H. F. Dacre (2009), Can dispersion model predictions be improved by increasing the temporal and spatial resolution of the meteorological input data?, Weather, 64, 232-237.

T. Davies, M. J. P. Cullen, A. J. Malcolm, M. H. Mawson, A. Staniforth, A. A. White and N. Wood (2004), A new dynamical core for the Met Office's global and regional modelling of the atmosphere, Q. J. R. Meteorol. Soc., 131, doi:10.1256/qj.04.101.

E. A. Donnell, D. J. Fish and E. M. Dicks (2001), Mechanisms for pollutant transport between the boundary layer and the free troposphere, J. Geophys. Res., 106(D8), 7847-7856.

B. Fay, H. Glabb, I. Jacobsen and R. Schrodin (1995), Evaluation of Eulerian and Lagrangian atmospheric transport models at the Deutscher Wetterdienst using ANATEX surface tracer data, Atmos. Env., 29, 2485-2497.

S. L. Gray (2003), A case study of stratospheric to troposphere transport: The role of convective transport and the sensitivity to model resolution, J. Geophys. Res., 108, 45990, doi:10.1029/2002JD003317.

D. Gregory and P. R. Rowntree (1990), A mass flux convection scheme with representation of cloud ensemble characteristics and stability dependent closure, Mon. Weather Rev., 118, 1483-1506.

G. A. Grell, R. Knoche, S. E. Peckham and S. A. McKeen (2004), Online versus offline air quality modeling on cloud-resolving scales, Geophys. Res. Letters, 31, doi:10.1029/2004GL020175.

S, -E, Gryning, E. Batchvarova, D. Schneiter, P. Bessemoulin and H. Berger (1998), Meteorological conditions at the release site during the two tracer experiments, Atmos. Env., 32, 4123-4137.

U. S. Korsholm, A. Baklanov, A. Gross and J. H. Sorensen (2009), On the importance of the meteorological coupling interval in dispersion modeling during ETEX-1, Atmos. Env., doi:10.1016/j.atmosenv.2008.11.017.

M. Krysta, M. Bocquet and J. Brandt (2008), Probing ETEX-II data set with inverse modelling, Atmos. Chem. Phys. Discuss., 8, 2795-2819.

A. P. Lock, A. R. Brown, M. R. Bush, G. M.Martin and R. N. B. Smith (2000), A new boundary layer mixing scheme. Part 1. Scheme description and single-column model tests, Mon. Weather Rev., 128, 187-199.

S. Mosca, G. Graziani, W. Klug, R. Bellasio and R. Bianconi (1998), A statistical methodology for the evaluation of long-range dispersion models: An application to the ETEX exercise, Atmos. Env., 32, 4307-4324.

J. S. Nasstrom and J. C. Pace (1998), Evaluation of the effect of meteorological data resolution on Lagrangian particle dispersion simulations using the ETEX experiment, Atmos. Env., 32, 4187-4194.

A. Priestley (1993), A quasi-conservative version of the semi-Lagrangian advection scheme, Mon. Wea. Rev., 121, 621-629.

P. J. Rasch, N. M. Mahowald and B. E. Eaton (1997), Representations of transport, convection, and the hydrologic cycle in chemical transport models: Implications for the modeling of short-lived and soluble species, J. Geophys. Res., 102, 28127-28138.

D. B. Ryall and R. H. Maryon (1998), Validation of the UK Met. Office's NAME model against the ETEX dataset, Atmos. Env., 32, 4265-4276.

B. A. Schichtel, M. G. Barna, K. A. Gebhart and W. C. Malm (2005), Evaluation of a Eulerian and Lagrangian air quality model using perfluorocarbon tracers released in Texas for the BRAVO haze study, Atmos. Env., 39, 7044-7062.

A. Stohl, M. Hittenberger and G. Wotawa (1998), Validation of the Lagrangian particle dispersion model FLEXPART against large-scale tracer experiment data, Atmos. Env., 32, 4245-4264.

H. Van Dop, R. Addis, G. Fraser, F. Girardi, G. Graziani, Y. Inoue, N. Kelly, W. Klug, A. Kulmala, K. Nodop and J. Pretel (1998), ETEX: A European tracer experiment; observations, dispersion modelling and emergency response, Atmos. Env., 32, 4089-4094.

D. R. Wilson and S. P. Ballard (1999), A microphsically based precipitation scheme for the UK Meteorological Office unified model, Q. J. R. Meteorol. Soc., 125, 1607-1636.